$$T = R_0,$$

where R_0 is the initial radius of the isolated circular domain.

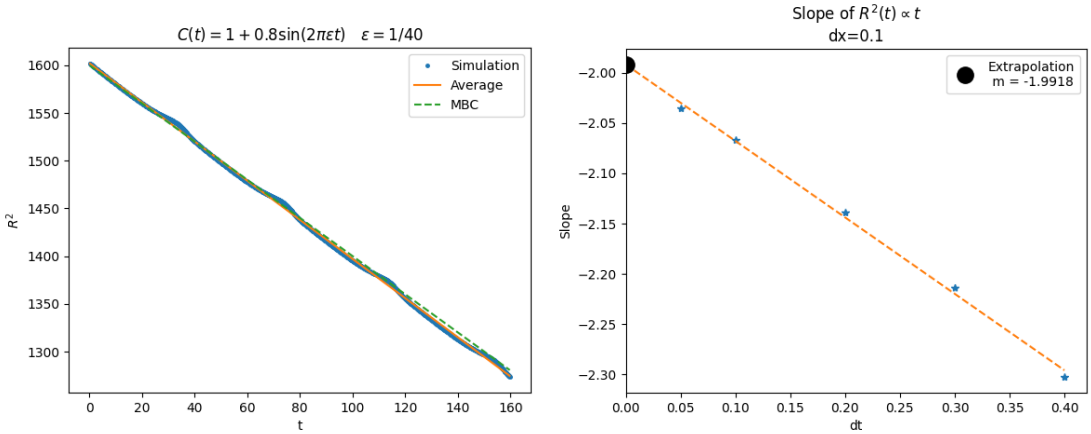

Figure 4.3: On the **left**: Square of the radius of an isolated circular domain $R(t)^2$ as a function of time, where $C(t) = 1 + 0.8\sin(2\pi\epsilon t)$ and $\epsilon = R(0)^{-1} = 1/40$. The blue curve correspond to the measured value of $R(t)^2$. The orange line is a time average, computed making a linear fit of the blue curve. While the green line corresponds to the expected relation if motion by curvature ($v = -\kappa$) holds: $R(t)^2 = R_0^2 - 2t$. The simulation parameters are $dt = 0.1$, $dx = 0.1$, $L = 128$, $R(0) = 40$. On the **right**: The simulation on the left was carried for multiple values of dt. Each time the slope of the experimental curve (the blue one) was estimated with a linear fit. Here the estimated slope is represented as a function of dt. A linear regression to extrapolate the slope value at $dt \to 0$ returns the value -1.992 ± 0.006, that is compatible with the expected value (-2) within two standard deviations.

In Figure 4.3 (left), the measured value of $R^2(t)$ during the simulation is plotted as a function of time. If motion by curvature is valid, we expect $R^2(t)$ to decay linearly, as demonstrated in Sec. 2.3:

$$R^2(t) = R_0^2 - 2t.$$

This linear decay is observed, particularly when the measures of $R^2(t)$ (shown by the blue curve) are averaged over time (orange line). However, the decay appears to be slightly faster than expected (green line).
This discrepancy can be attributed to the discreteness of time steps used in the simulations. To address this, Figure 4.3 (right) illustrates the estimation of the slope of the orange curve by running simulations with various time step values dt. An extrapolation to $dt \to 0$ confirms the expected value of the slope, thereby validating the motion by curvature behavior in the simulations.

4.3.2 Fast varying temperature

This scenario represents the opposite limit, where the time scale associated with the variations of $C(t)$ is one order of magnitude larger than the intrinsic time scale

τ_{linear}. To analyze this, we introduce the time variables:

$$t_{-1} = \epsilon^{-1}t; \quad t_0 = t; \quad t_1 = \epsilon t.$$

In this limit, we define $C(t)$ as follows:

$$C(t) = C_0 + D_0(t_{-1}),$$

where C_0 is the average value of $C(t)$ and $D_0(t_{-1})$ represents an oscillation around zero with period T:

$$\int_{t_{-1}}^{(t_{-1}+T)} D_0(t'_{-1})dt'_{-1} = 0 \quad \forall t_{-1}.$$

Consequently, we have

$$\partial_{t_0} C = \partial_{t_1} C = 0,$$

while in general, the time derivative can be expressed as:

$$\partial_t = \epsilon^{-1}\partial_{t_{-1}} + \partial_{t_0} + \epsilon\partial_{t_1}.$$

It is important to note that this small parameter ϵ is the same one that appears in the equations 4.3.1, 4.3.2, and 4.3.3; it characterizes the smallness of the curvature of an interface.
Following the same approach used in the analysis of the slow-varying $C(t)$ limit, we incorporate the interface propagation phenomena into the time derivative as follows:

$$\partial_t = \epsilon^{-1}\partial_{t_{-1}} + \partial_{t_0} + \epsilon\partial_{t_1} - \epsilon V_1\partial_\xi. \tag{4.3.9}$$

Next, we expand the state in powers of ϵ:

$$m(x,t) = m_0(x,t) + \epsilon m_1(x,t) + \epsilon^2 m_2(x,t) + O(\epsilon^3).$$

By substituting this expansion, along with Equations 4.3.1, 4.3.2, and 4.3.9, into the two-dimensional TDGL equation

$$\partial_t m = \Delta m + C(t)m - m^3,$$

we obtain

$$\epsilon^{-1}\partial_{t_{-1}}m_0 + \partial_{t_0}m_0 + \partial_{t_{-1}}m_1 + \epsilon(\partial_{t_0}m_1 + \partial_{t_{-1}}m_2 + \partial_{t_1}m_0 - V_1\partial_\xi m_0) =$$
$$= \partial_{\xi\xi}m_0 + (C_0 + D_0(t_{-1})m_0 - m_0^3 + \epsilon[\partial_{\xi\xi}m_1 + K_1\partial_\xi m_0 + (C_0 + D_0(t_{-1})m_1 - 3m_0^2 m_1] + O(\epsilon^2)$$

Equating the terms of order ϵ^{-1} we find

$$\partial_{t_{-1}}m_0 = 0$$

while for the order ϵ^0 we find

$$\partial_{t_{-1}}m_1 + \partial_{t_0}m_0 = (C_0 + D_0(t_{-1}))m_0 - m_0^3 + \partial_{\xi\xi}m_0$$

The last two equations, are the same ones we found in the 1D analysis of the fast varying $C(t)$ limit, where $x \to \xi$. In that analysis, these equations led to Eq. 4.2.11 and Eq. 4.2.13, that we recall

$$m_0 = \sqrt{C_0}\tanh\left(\xi\sqrt{\frac{C_0}{2}}\right)$$

$$m_1 = m_0(\xi)\int_{\tau_{-1}(t_0,t_1,\xi)}^{t_{-1}} D_0(t'_{-1})dt'_{-1} \tag{4.3.10}$$

where during the 1D analysis we couldn't determine $\tau_{-1}(t_0, t_1, \xi)$ due to lack of additional equations. As we're interested in the motion of the interfaces, that is a first order (ϵ^1) phenomena, this time we consider also the equation associated with order ϵ^1

$$\partial_{t_{-1}}m_2 + \partial_{t_0}m_1 + \partial_{t_1}m_0 - V_1\partial_\xi m_0 = (C_0 + D(t_{-1}))m_1 - 3m_0^2m_1 + \partial_{\xi\xi}m_1 + K_1\partial_\xi m_0$$

We know that $m_0 = m_0(\xi)$, so $\partial_{t_1}m_0 = 0$. We then make the following assumption to solve the equation. Although we were unable to fully interpret its physical significance, it simplifies the equation, enabling us to find a solution, even if it is not the most general one.

$$\partial_{t_0}\tau_{-1} = \partial_\xi\tau_{-1} = 0$$

Which implies, using Eq. 4.3.10

$$\partial_{t_0}m_1 = 0$$

$$\partial_{\xi\xi}m_1 = \partial_{\xi\xi}m_0\int_{\tau_{-1}}^{t_{-1}} D_0(t'_{-1})dt'_{-1}$$

As a consequence, the equation associated with order ϵ^1 becomes

$$\partial_{t_{-1}}m_2 - V_1\partial_\xi m_0 = (C_0 + D(t_{-1}))m_1 - 3m_0^2m_1 + \partial_{\xi\xi}m_0\int_{\tau_{-1}}^{t_{-1}} D_0(t'_{-1})dt'_{-1} + K_1\partial_\xi m_0$$

$$\partial_{t_{-1}}m_2 = [(C_0m_0 + D_0(t_{-1})m_0 - 3m_0^2 + \partial_{\xi\xi}m_0]\int_{\tau_{-1}}^{t_{-1}} D_0(t'_{-1})dt'_{-1} + (V_1 + K_1)\partial_\xi m_0$$

Remembering that $m_0(\xi)$ is a stationary solution of the 1D TDGL equation with $C = C_0$ constant, it holds

$$C_0m_0 - m_0^3 + \partial_{\xi\xi}m_0 = 0$$

And using this statement in the previous equation

$$\partial_{t_{-1}}m_2 = [D_0(t_{-1})m_0 - 2m_0^3]\int_{\tau_{-1}}^{t_{-1}} D_0(t'_{-1})dt'_{-1} + (V_1 + K_1)\partial_\xi m_0 \tag{4.3.11}$$

To derive a formula for the interface velocity V_1, we must introduce an additional assumption. We anticipate that the order parameter u remains bounded at all times.

Since m_0 does not depend on time and m_1 is periodic—due to the periodic nature of $D_0(t_{-1})$. We also assume that m_2 is periodic with the same period as $D_0(t_{-1})$:

$$m_2(t_{-1} + T) = m_2(t_{-1}).$$

This periodicity leads to the condition:

$$\Delta m_2 \equiv \int_{\tau_{-1}}^{\tau_{-1}+T} \partial_{t'_{-1}} m_2(t'_{-1})\, dt'_{-1} = 0.$$

We can use this last statement if we integrate $\int_{\tau_{-1}}^{\tau_{-1}+T} dt_{-1}$ the Eq. 4.3.11

$$\mathbf{0} = m_0 \int_{\tau_{-1}}^{\tau_{-1}+T} D_0(t_{-1})dt_{-1} \int_{\tau_{-1}}^{t_{-1}} D_0(t'_{-1})dt'_{-1} + \tag{4.3.12}$$

$$-2m_0^2 \int_{\tau_{-1}}^{\tau_{-1}+T} dt_{-1} \int_{\tau_{-1}}^{t_{-1}} D_0(t'_{-1})dt'_{-1} + (V_1 + K_1)\partial_\xi m_0 T$$

Next, we observe that we have a sum of three terms that depend on ξ in different ways: specifically, as m_0, m_0^2, and $\partial_\xi m_0$. Since the equation must hold for all ξ, each of these three terms must individually be zero for their sum to equal zero.
It follows that

$$(V_1 + K_1)\partial_\xi m_0 T = 0 \quad \forall \xi \tag{4.3.13}$$

so we find the usual equation for motion by curvature

$$V_1 = -K_1$$

. We couldn't prove rigorously this statement, however we can at least prove (in Appendix F) that is exists a value for τ_{-1} such that Eq. 4.3.12 reduces to Eq. 4.3.13. This result tells that, up to leading order, motion by curvature is not affected by a time dependent $C(t)$.

Numerical evidence

Similar to our analysis in the opposite limit, we verified the motion by curvature relation $v = -\kappa$ by simulating the dynamics of an isolated circular domain. For the time dependence of $C(t)$, we used the expression

$$C(t) = \bar{C} + A \sin\left(2\pi \frac{t}{T}\right).$$

In the previous case, we established that $T \sim \epsilon^{-1}$ since $C(t)$ was slowly varying over time. In this instance, however, the time scale describing the variation must be small, so we set $T \sim \epsilon$. Consequently, we make the following choice for the initial radius:

$$T = R_0^{-1}.$$

A simulation of this type is presented in Figure 4.4. The results validate the analytical analysis, confirming that motion by curvature serves as the driving mechanism of the dynamics when $C(t)$ varies rapidly over time.

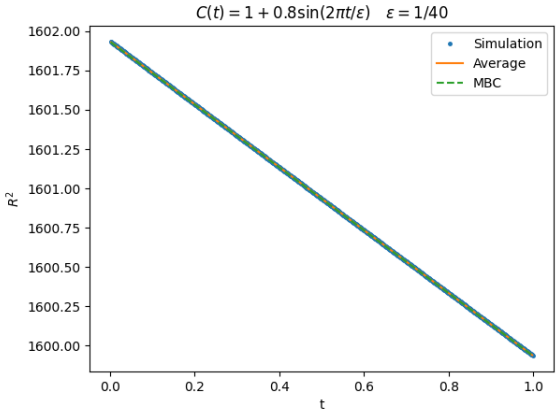

Figure 4.4: Square of the radius of an isolated circular domain $R(t)^2$ as a function of time, where $C(t) = 1 + 0.8\sin(2\pi t/\epsilon)$ and $\epsilon = R(0)^{-1} = 1/40$. The blue curve corresponds to the measured value of $R(t)^2$. The orange line is a time average, computed making a linear fit of the blue curve. While the green line corresponds to the expected relation if motion by curvature ($v = -\kappa$) holds: $R(t)^2 = R_0^2 - 2t$. The simulation parameters are $dt = 0.1$, $dx = 0.1$, $L = 128$, $R(0) = 1/40$.

4.3.3 Controlling the coarsening dynamics

In the previous sections, we numerically verified the motion by curvature relation $v = -\kappa$ by examining the dynamics of a specific system initially prepared with a single isolated circular domain. However, as discussed in Sec. 2.3.2, starting from random initial conditions, the number of domains decreases asymptotically while their average size increases as a power law of time, specifically $\ell \sim t^{\frac{1}{2}}$. We motivated this behavior, known as coarsening dynamics, by applying the motion by curvature relation $v = -\kappa$ within a dimensional analysis framework. This indicates that motion by curvature can be validated by observing that the typical size of the domains grows as a power law over time, particularly with an exponent of $\ell \sim t^{\frac{1}{2}}$.
In this section, we will present simulations of the asymptotic dynamics in the two distinct limits where the time variations of $C(t)$ are either slow or fast relative to the intrinsic timescale of the system. In both scenarios, we will demonstrate that the coarsening dynamics remains unaffected by a time-dependent $C(t)$. Specifically, we'll verify that the characteristic power-law growth of domain size, $\ell \sim t^{\frac{1}{2}}$, persists regardless of whether $C(t)$ changes slowly or rapidly over time.
As in the previous section, we adopted a time-dependent $C(t)$ given by

$$C(t) = \bar{C} + A\sin\left(2\pi\frac{t}{T}\right)$$

In the slow-varying limit, the period T of $C(t)$ is much larger than the intrinsic timescale of the system, $\tau_{\text{linear}} \sim \frac{1}{\bar{C}}$ (which is approximately 1, since $\bar{C} = 1$). Specifically, we chose $T = 25 \gg 1$ to represent this slow-varying case.
Conversely, to study the fast-varying limit of $C(t)$, we set $T = 0.025 \ll 1$, such that the period of $C(t)$ is much smaller than the system's intrinsic timescale.
In Figure 4.5, we present the results of two simulations illustrating how the average